Available online at www.sciencedirect.com

SciVerse ScienceDirect

Journal of the European Ceramic Society 32 (2012) 559–567

www.elsevier.com/locate/jeurceramsoc

Glass additive in barium titanate ceramics and its influence on electrical breakdown strength in relation with energy storage properties

Xiangrong Wang, Yong Zhang *, Xiaozhen Song, Zongbao Yuan, Tao Ma, Qian Zhang, Changsheng Deng, Tongxiang Liang

Beijing Fine Ceramics Laboratory, State Key Laboratory of New Ceramics and Fine Processing, Institute of Nuclear and New Energy Technology, Tsinghua University, Beijing 100084, PR China

Received 29 July 2011; received in revised form 22 September 2011; accepted 26 September 2011
Available online 21 October 2011

Abstract

Glass additive was employed to improve the microstructures and energy storage properties of barium titanate ceramics using liquid phase sintering technology. Microstructural observation indicated that the average grain size reduced obviously with increasing glass concentration. Also, the dielectric constant decreased and the dielectric breakdown strength increased as glass concentration increased. The increase in the breakdown strength with decreasing grain size was consistent with the well-known relationship for the mechanical failure. The activation energies of bulk grain and grain boundary as well as their differences were calculated using measured impedance values. Good inverse dependence of the dielectric breakdown strength on the difference between activation energies of bulk grain and grain boundary was obtained for the glass-added $BaTiO_3$ ceramics. It was also found that the energy storage density of the ceramics increased gradually with increasing glass concentration. Possible effect of the interfacial polarization in degrading the energy storage property was discussed.

Keywords: Sintering; Grain size; Dielectric properties; Glass; $BaTiO_3$; Titanates

1. Introduction

Barium titanate ($BaTiO_3$) ceramics have been highlighted over the past five decades as dielectric materials in capacitors, because of their high dielectric constants. Both the increasing reliability of electronic packages incorporating ceramic capacitors[1] and high energy density application[2] have led to increasing concern over their dielectric breakdown strengths. In recent years, there has been a lot of interest in high energy density capacitors since their indispensable functions can be utilized for filtering, coupling, snubbing and dc blocking in power electronic circuits. High dielectric breakdown strengths are critical in determining the energy storage capability of dielectric materials. Therefore, numerous investigations on $BaTiO_3$ ceramics have focused on their high breakdown strengths.

The dielectric breakdown strength (BDS) of ceramics is well known to be substantially influenced by several factors, such as porosity,[3] grain size,[4,5] introduction of second phase,[6] temperature, charge injection[7] and interfacial polarization.[8] Porosity appears to be a dominant factor in affecting the BDS. The lack of control over the densities of $BaTiO_3$ ceramics results in microstructural variations that lead to poor breakdown property optimization and reproducibility. The inability to produce the ceramics with high densities limits the energy storage capability, thereby limiting the level of device miniaturization possible in the capacitive storage based pulse power systems.

The slurry of attention given to the BDS justifies a great need to develop processing method for high density ceramics. Liquid phase sintering technology, which enables the preparation of ideal density with little or no porosity, has been studied extensively. The key features investigated include the additive of a fluxing agent, such as glass, to $BaTiO_3$ powders and the effects of glass composition and concentration on densifications,[3] microstructures,[5] dielectric properties, and

* Corresponding author. Tel.: +86 10 80194055; fax: +86 10 89696022.
E-mail address: yzhang@tsinghua.edu.cn (Y. Zhang).

0955-2219/$ – see front matter © 2011 Elsevier Ltd. All rights reserved.
doi:10.1016/j.jeurceramsoc.2011.09.024

energy storage densities.[2] Sarkar and Sharma[9] presented the effects of adding 2–20 mol% B_2O_3 and PbB_2O_4 glasses on the BDS and the dielectric constant of $BaTiO_3$ and observed an increase in the BDS by a factor of 2 and a decrease in the dielectric constant (1500–700). Young et al.[5] studied the effect of a $BaO–SiO_2–B_2O_3$ glass additive on the BDS of $BaTiO_3$ ceramics and demonstrated that the BDS of the samples containing 20 vol% glass was enhanced 2.8 times. Recently, it was reported that the energy storage density of $Ba_{0.4}Sr_{0.6}TiO_3$ ceramics with 5 vol% $BaO–SiO_2–B_2O_3$ glass additive was improved by a factor of 2.4 compared with that of pure $Ba_{0.4}Sr_{0.6}TiO_3$ ceramics.[10]

In addition, microstructural evaluations are not enough to elucidate the mechanism responsible for the dielectric breakdown. Recent work[7] investigating the relationships between dielectric breakdown resistance and charge transport in alumina materials determined that the good breakdown resistance depends on charge transport behaviors. These main behaviors associated with breakdown improvement are (i) diffusion of charge, (ii) trapping limiting injection, and (iii) trapping in surface phases with instantaneous electron reemission. The charge diffusion model predicts the BDS will be improved if the ceramics are able to stabilise a great amount of charges. When the temperature increases, the traps hindering the charge spreading can decrease, thereby improving the ability of the charges to diffuse within the materials.

In the present work, we have studied the influence of a specific glass additive ($BaO–SrO–TiO_2–Al_2O_3–SiO_2–BaF_2$) on the microstructures, dielectric breakdown strengths and energy storage properties of $BaTiO_3$ ceramics. Firstly, we will report and discuss the microstructural evolution with increasing glass additive, as well as the influence on the dielectric constant and the BDS. We will show that there is a relationship[4,5] of $BDS \propto d^{-1/2}$ (where d denotes the grain size) established in these glass-added $BaTiO_3$ ceramics. Then, we will perform the impedance analysis on the same samples. It will be shown that the impedance semicircles are sensitive to the amounts of glass additive. These results will raise questions concerning the correlation between BDS and activation energy. Finally, we will investigate the energy storage properties measured by the use of the Sawyer–Tower circuit in conjunction with the variation of glass additive.

2. Experimental procedures

The materials studied here are glass-added $BaTiO_3$ ceramics which have been formulated utilizing different glass concentrations. The base $BaTiO_3$ is a commercially available material already in use in the manufacturing of capacitors. The additive is an aluminum silicate glass from which a perovskite phase could crystallize at about 850 °C during heat treatment.[11]

2.1. Glass additive fabrication

The composition of this specific glass is 27.68 $BaCO_3$–6.92 $SrCO_3$–29 TiO_2–22 SiO_2–12 Al_2O_3–2.4 BaF_2 (mol%). A powder containing appropriate constituents was ball-milled for 4 h in a high density polyethylene bottle with deionized water as milling media for homogenous mixing. After dried at 100 °C for 2 h, the powder was placed in a platinum crucible and heated to 1550 °C in a box furnace to sequentially decompose the carbonates and to melt the constituent powders to a viscous liquid. The melt was homogenized at 1550 °C for 2 h, and then quickly removed from the furnace to be poured into water to get glass powder. Subsequently the glass frit was ball-milled for 10–12 h and then sieved to pass through a 60 mesh screen to produce powders of fine particle size.

2.2. Sample preparation

Hydrothermally derived $BaTiO_3$ powder used throughout this study was supplied by Guoteng Co. Ltd., Shandong, China and its average particle size was approximately 100 nm. The glass frit was mixed in ratio corresponding to the following chemical composition: $(100 - x)$ wt% $BaTiO_3 + x$ wt% glass, where $x = 4$ (BT-G4), $x = 5$ (BT-G5), $x = 6$ (BT-G6), and $x = 7$ (BT-G7), respectively. The weighed $BaTiO_3$ and glass frit powders were thoroughly wet-milled for 24 h in a ball mill with the addition of alcohol and zirconia as the milling media and then the obtained slurry was dried in an oven. After drying, these homogeneous mixtures were sieved. To prepare the powders for pressing, they were mixed with 3 wt% PVA solution, pulverized using a mortar and pestle, and then pressed into pellets of 10 mm in diameter and 0.7 mm in thickness under a uniaxial pressure of 4 MPa. After de-binding, these pellets were sintered in air at temperatures from 1050 to 1180 °C for 2 h using a heating rate of 5 °C/min.

2.3. Characterization

The bulk densities of the sintered samples were measured by the Archimedes method with an immersion medium of distilled water. The diameter shrinkages were measured by a

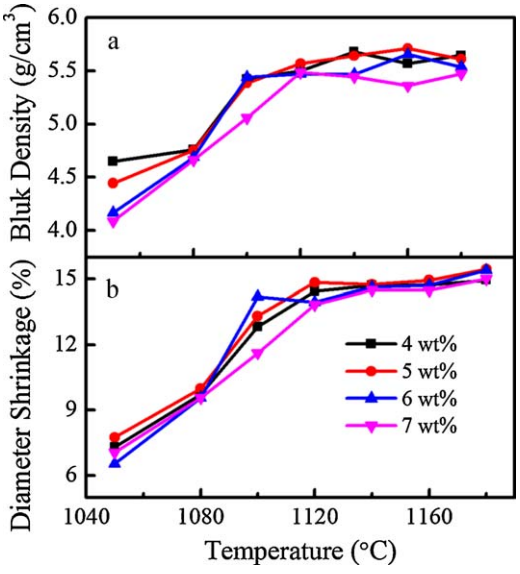

Fig. 1. Bulk density and diameter shrinkage as a function of sintering temperature for the glass-added $BaTiO_3$ ceramics.

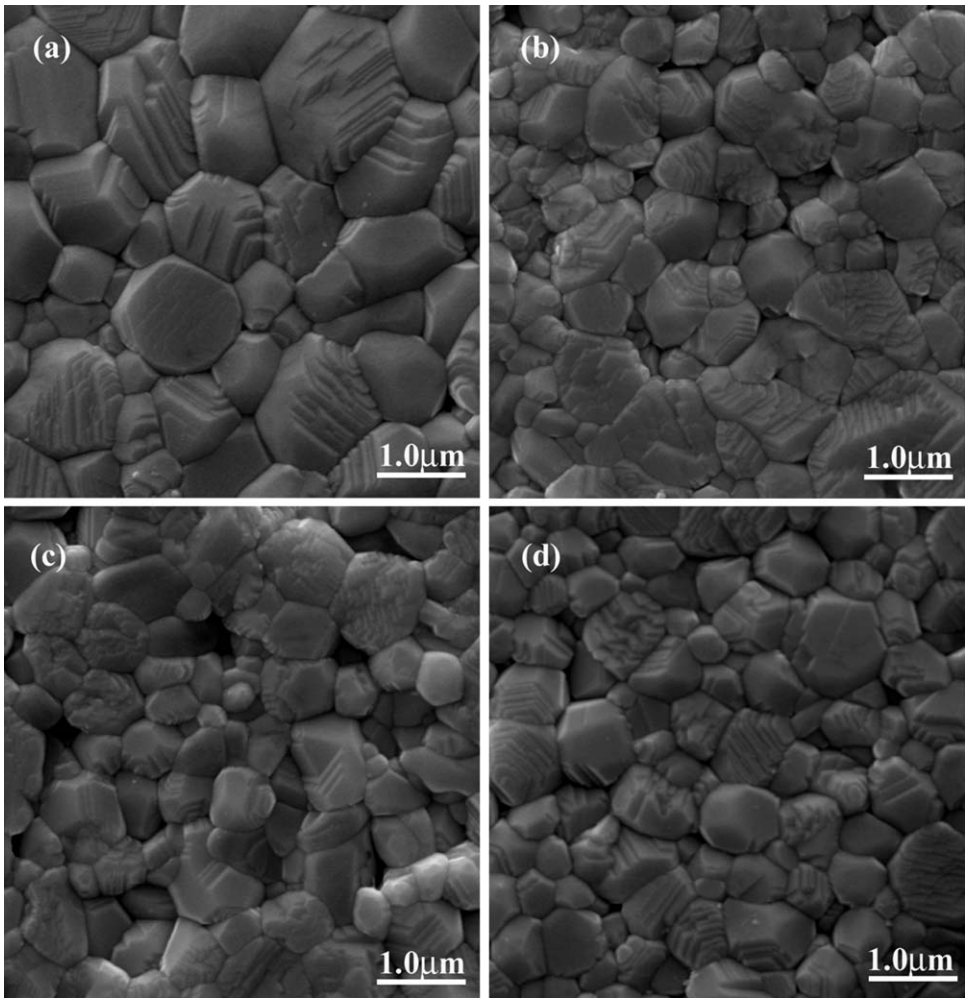

Fig. 2. SEM micrographs of the $BaTiO_3$ ceramics with different amounts of glass additive. (a) BT-G4; (b) BT-G5; (c) BT-G6; (d) BT-G7.

micrometer. The polished and thermal-etched surfaces of the sintered samples were examined using field emission scanning electron microscopy (Model Quanta 200 FEG, FEI, Eindhoven, the Netherlands). The average grain size has been obtained by using image analysis techniques and reported here with an accuracy of ±5% at 95% confidence level. The sintered samples were painted with silver paste on both sides and fired at 550 °C for 20 min to prepare electrodes for dielectric measurements. The dielectric response was performed using impedance analyzer (Model HP4284A, Hewlett-Packard, Palo Alto, CA) interfaced with a computer controlled temperature chamber in the temperature range of −50 to 150 °C with the measuring frequency of 20 Hz to 1 MHz. The disk-shaped specimens were used to measure the dc breakdown strength with a high-voltage source HF5013 K (Huiyou Electronics Co. Ltd., Changzhou, China) using a voltage ramp rate of about 1 kV/s at ambient temperature. All samples were immersed in silicon oil to prevent flashover and corona discharge. The measured dielectric breakdown strength values were ranked and the probability of failure P_i was calculated using the following formula:

$$P_i = \frac{i}{n+1} \tag{1}$$

where i is the ith sample to be ranked and n is the sum of specimens tested. A statistical distribution commonly used to represent the strength of brittle materials is proposed by Weibull.[12] And the breakdown strength of the glass-added $BaTiO_3$ ceramics was evaluated by the two-parameter Weibull analysis, [8,11,13]

$$P_i = 1 - \exp\left[-\left(\frac{E_i}{E_b}\right)\right]^{\beta} \tag{2}$$

where E_i is the measured breakdown strength for the ith specimen in the experiments, E_b is the characteristic breakdown strength, β is the shape parameter. Complex impedance spectrum were carried out at an input signal level of 4 V in a wide temperature range of 350 to 530 °C using a computer-controlled impedance analyzer, in the frequency range of 20 Hz to 1 MHz.

The polarization–electric field (P–E) hysteresis loops were measured at room temperature and a frequency of 1 Hz by a modified Sawyer–Tower bridge. The energy storage density of the glass-added $BaTiO_3$ ceramics could be calculated from the P–E hysteresis loop. The energy density is given by

$$J = \int_0^{P_{\max}} E\,dP \tag{3}$$

where E is the strength of electric field and P_{max} is the electric polarization at the highest applied field E_{max}. The energy density charged is equal to integral of the area enclosed by charge curve and y-axis. The energy density discharged is equal to integral of the area enclosed by discharge curve and y-axis. The unreleased energy density or the energy loss is equal to integral of the area enclosed by charge and discharge curve and y-axis.

3. Results

The effect of sintering temperature on bulk density and diameter shrinkage in the glass-added $BaTiO_3$ ceramics is shown in Fig. 1. It indicates that as the sintering temperature increases in the interval from 1050 to 1120 °C, both the bulk density and the diameter shrinkage of each composition show a drastic increase. Further increase in sintering temperature does not result in the apparent change in the bulk density and the diameter shrinkage of the glass-added samples. Thus, for each of these four compositions, the highest bulk density and diameter shrinkage can be obtained at 1180 °C for 2 h.

In addition, the variations of the bulk density and the diameter shrinkage with glass concentration are also shown in Fig. 1. There is slight variation in the bulk density and the diameter shrinkage of the glass-added samples with increasing glass concentration.

The SEM micrographs of $BaTiO_3$ ceramics added with different amounts of glass additive sintered at 1180 °C for 2 h were shown in Fig. 2. The specimens were thermally etched for 15 min at 1130 °C after being polished. It can be seen that a mixture of various grain sizes is evident for 4 wt% glass-added $BaTiO_3$ ceramic samples, which show very large grains coexist with very small ones. With increasing glass concentration, the average grain size decreased gradually. Thus, it can be seen that glass additive is also effective to decrease grain size and improve the microstructure homogeneity.

Fig. 3 plots the average grain size as a function of glass concentration. The average grain size for the 4 wt% glass-added sample is about 0.80 μm, and decreases with increasing glass concentration to minimum value of approximately 0.46 μm for the 7 wt% glass-added samples. Thus, SEM study of the microstructure revealed that this specific glass additive plays an important role in controlling grain growth.

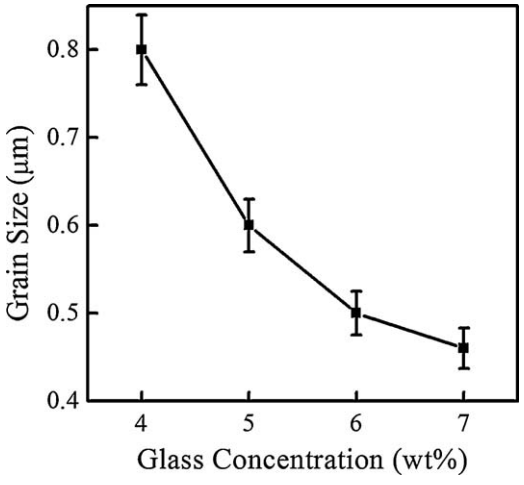

Fig. 3. Average grain size as a function of glass concentration. Error bars represent ±2 standard deviation about the mean.

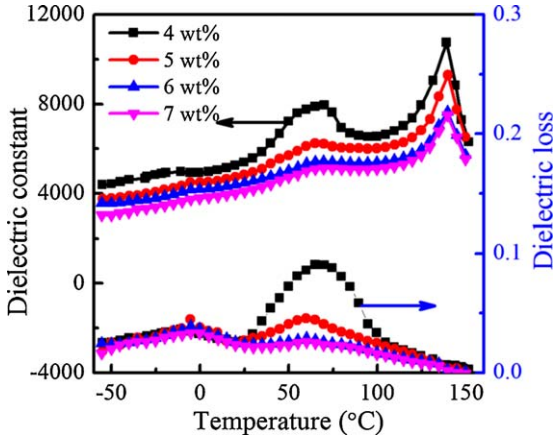

Fig. 4. Temperature dependences of dielectric constant and dielectric loss of the $BaTiO_3$ ceramics added with different amounts of glass additive. Measurement frequency for each sample was 1 kHz.

The influence of glass concentration on the dielectric–temperature characteristics of the $BaTiO_3$ ceramics over the temperature range of −50 to 150 °C was illustrated in Fig. 4. The dielectric constant decreases as the glass content increases. Plots of the dielectric constant versus temperature comprise two maxima, one situated in the region of 50–70 °C (lower temperature regime) and the other at about 130 °C (higher temperature regime). Both the two dielectric constant maxima at the two temperature regimes systematically decrease as the glass content decreases. Close inspection of the lower transition temperature revealed there is an increase in dielectric loss with decreasing glass content. This result was related to interfacial polarization. However, there is no obvious change in dielectric loss with glass content for the higher transition temperature, which is attributed to ferroelectric–paraelectric phase transition in the $BaTiO_3$ ceramics.

The dielectric breakdown strength (BDS) of glass ceramics under some condition is found to follow, both in theory and in practice, the Weibull distribution. Fig. 5 illustrates the Weibull plot of the BDS for the glass-added $BaTiO_3$ ceramic samples. As seen from Fig. 5, all the samples exhibit qualitatively similar behavior, and the data are almost linear indicating that the characteristic breakdown strength are adequately described by a two-parameter Weibull distribution. Fig. 6 shows the characteristic breakdown strength of the glass-added $BaTiO_3$ ceramic as a function of glass additive. Within this glass additive range, the dielectric breakdown strength increases gradually with glass additive and rises from 7.02 kV/mm for the 4 wt% glass-added samples to 9.46 kV/mm for the 7 wt% glass-added samples.

Impedance analysis was performed to study the effect of glass additive on the dielectric properties of the glass-added $BaTiO_3$ ceramics. Fig. 7 gave the complex impedance spectra measured at 380 °C for the specimens with different glass concentrations. It can be seen that the complex impedance plots display only one strongly suppressed semicircle which can be associated with a

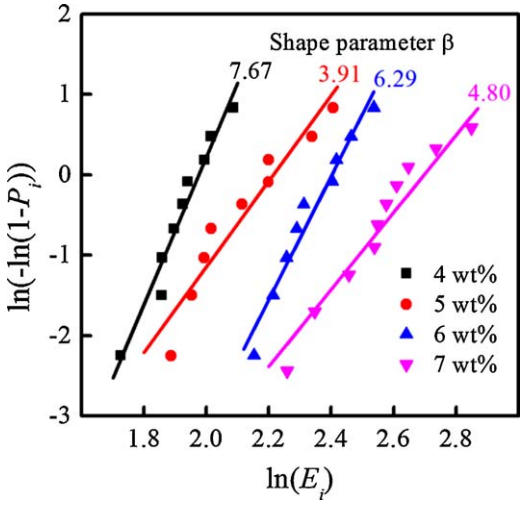

Fig. 5. A Weibull plot indicating the failure distribution for $BaTiO_3$ ceramics added with different amounts of glass additive.

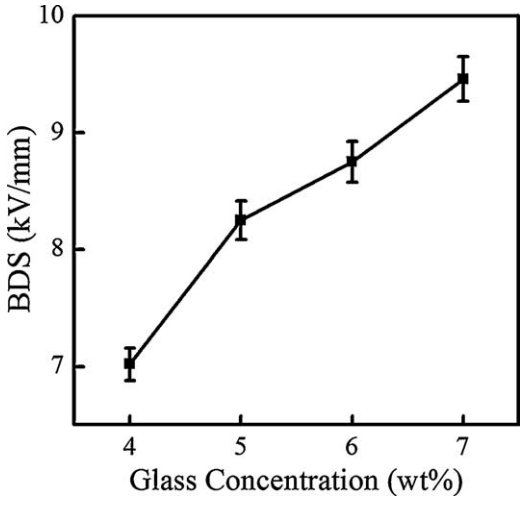

Fig. 6. BDS as a function of glass concentration. Error bars represent ±2 standard deviation about the mean.

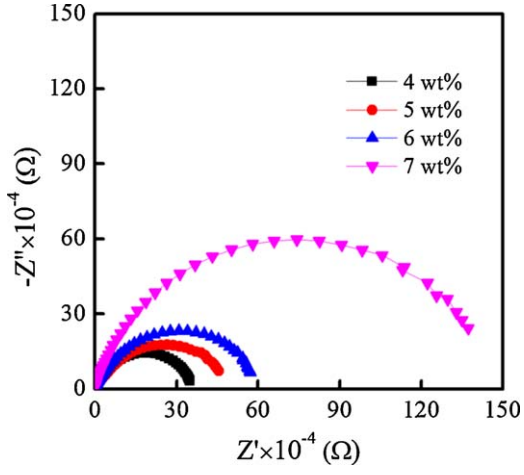

Fig. 7. Complex impedance spectra at 380 °C for the $BaTiO_3$ ceramics added with different amounts of glass additive.

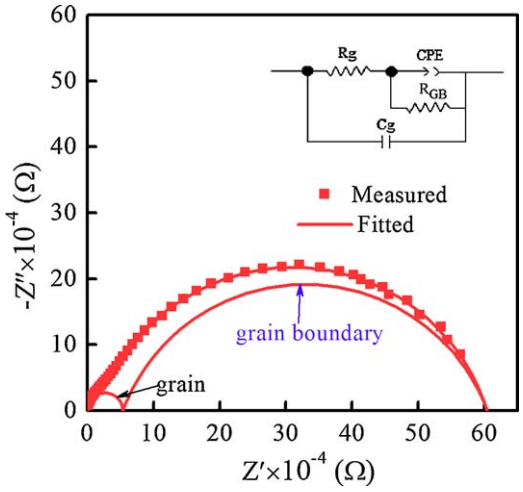

Fig. 8. Complex impedance spectra of measured (red filled squares) and fitted (red line) data at 380 °C for the $BaTiO_3$ ceramics with 5 wt% glass. The inset shows an equivalent circuit for the $BaTiO_3$ ceramic system, where the circuit elements R_g-C_g and R_{GB}-CPE represent the contributions from the grain and grain boundary, respectively. (For interpretation of the references to colour in this figure legend, the reader is referred to the web version of this article.)

strong overlap of two semicircles due to similar relaxation time constant τ of the two relaxation processes. And the impedance semicircles become larger with increasing glass concentration.

Fig. 8 gives complex impedance plot of experimental (red filled squares) and fitting (red line) data at 380 °C for the 5 wt% glass-added $BaTiO_3$ ceramics. It is shown that a simple equivalent circuit allows a good fitting with experimental data. According to the general explanation of the impedance analysis,[14] the small arc can be attributed to the contribution of bulk *RC* network, where *R* is resistance, *C* is capacitance, and the large arc at low frequencies is attributed to the contribution of the grain boundary *RQ* network where *Q* is constant phase element.

By fitting the measured impedance data using the equivalent circuit shown in the inset of Fig. 8 itself, the capacitance value can also be obtained from the following equation[15,16]:

$$C = (R^{1-n}Q)^{1/n} \tag{4}$$

where n is the relaxation distribution parameter, $n=1$ for a pure capacitor, $n=0$ for a pure resistor and $n=0.5$ for a Warburg impedance (pure diffusion).The relaxation time of bulk (τ_g) and grain-boundary (τ_{GB}) is defined as:

$$\tau_g = R_g C_g \tag{5}$$

$$\tau_{GB} = R_{GB} C_{GB} \tag{6}$$

The variation of relaxation time as a function of temperature is illustrated in Fig. 9. The relaxation time was obtained from the nonlinear least squares fitting of the complex impedance data measured at various temperatures using Eqs. (4)–(6). The relaxation time decreases with the increasing temperature, as

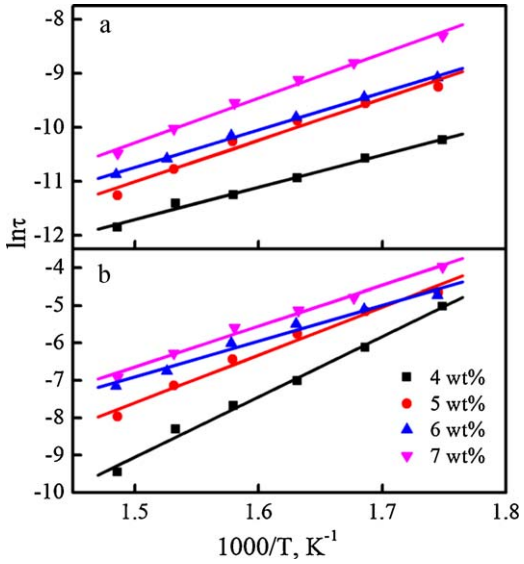

Fig. 9. The relaxation time of grain (a) and grain boundary (b) as a function of $1000/T$ for the glass-added $BaTiO_3$ ceramics.

shown in Fig. 9. And it can be seen that plots of $\ln \tau$ versus $1/T$ are linear and obey the Arrhenius relationship.[8]

$$\tau = \tau_0 \exp\left(-\frac{\phi}{kT}\right) \quad (7)$$

where τ is the relaxation time, τ_0 is the pre-exponential factor, ϕ is the activation energy, k is the Boltzmann constant, and T is the absolute temperature.

The value of activation energy suggests that the associated relaxation processes originate from some kind of charge carriers. Thus, according to Eq. (7), the calculated activation energies of the glass-added $BaTiO_3$ ceramics can be obtained from the slope of the function between relaxation time and measuring temperature shown in Fig. 10.

The glass concentration dependence of the activation energies of bulk and grain boundary was shown in Fig. 10. As seen from Fig. 10, the grain boundary activation energy decreases from 1.33 eV to 0.84 eV in the glass concentration range of 4–6 wt%, and then increases up to 0.93 eV at the glass concentration of 7 wt%, while bulk activation energy slightly changes between 0.48 eV and 0.61 eV, which indicate that bulk and grain boundary have different electrical transport characteristics.

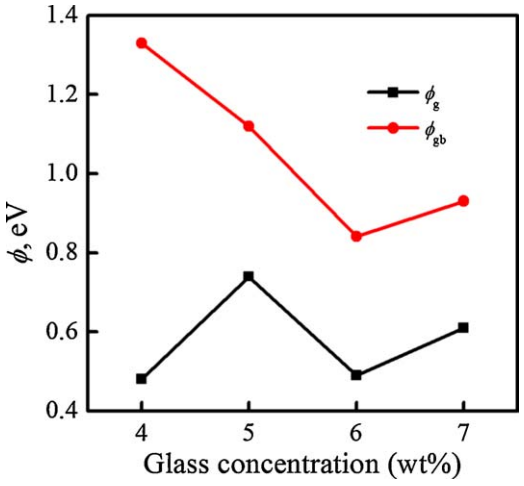

Fig. 10. The activation energies of grain and grain boundary for the $BaTiO_3$ ceramics with different amounts of glass additive.

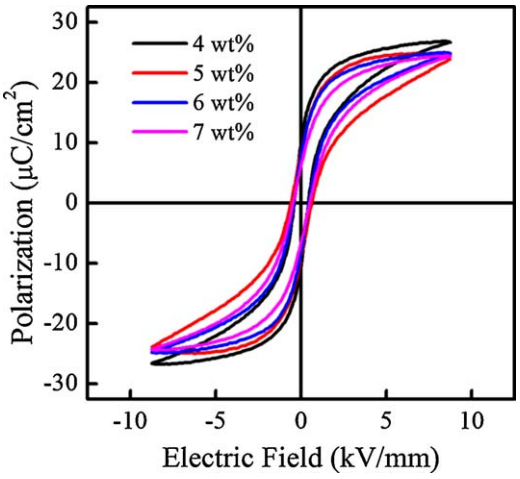

Fig. 11. Polarization–electric field hysteresis loops for the $BaTiO_3$ ceramics added with different amounts of glass additive.

The *P–E* hysteresis loop measurements using the Sawyer–Tower circuit were made on the glass-added $BaTiO_3$ ceramics fabricated in this study to examine their energy storage properties. Fig. 11 shows the glass concentration dependence of *P–E* hysteresis loops for the glass-added $BaTiO_3$ ceramics. It can be seen that the maximum polarization of the glass-added $BaTiO_3$ ceramics is about 24–27 $\mu C/cm^2$ and the remnant polarization is basically decreased with the increase of glass additive.

In general, the stored electric energy density of a dielectric material can be evaluated from the area by integrating the discharge curve in the *P–E* hysteresis loop within the interval of polarization from P_{min} ($E = 0$ kV) to P_{max} ($E = 8.8$ kV). So the energy densities calculated from *P–E* hysteresis loops were shown in Fig. 12. As seen from Fig. 12, among all the measured

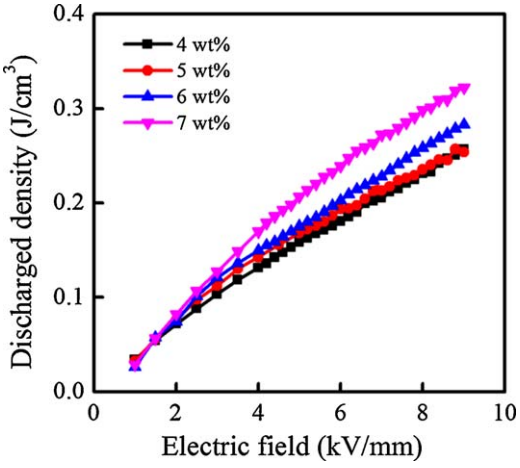

Fig. 12. Electric field dependence of discharged energy density of the $BaTiO_3$ ceramics added with different amounts of glass additive.

samples, BT-G7 has the highest energy density of 0.32 J/cm^3, which is 1.3 times higher than that of BT-G4. And the energy density of $BaTiO_3$ ceramics increases with increasing glass content. The results indicate that the increase of BDS and the mitigation of interface polarization may result in the improvement of energy density in the glass-added $BaTiO_3$ ceramics.

4. Discussion

All the above-mentioned microstructures and dielectric properties in the glass-added $BaTiO_3$ ceramics demonstrated glass concentration dependences. In this section, we will first discuss two contributions for the BDS results obtained for the various glass concentrations and will then compare the energy storage results.

4.1. Grain size contribution

Taking into account that the glass system developed as sintering aids for $BaTiO_3$ may not only act as a fluxing agent for sintering but also as a modifier of the dielectric properties if the glass component is incorporated into the $BaTiO_3$ lattice, we chose the specific aluminum silicate glass system. During the heat treatment, the crystallization of (Ba, Sr)TiO_3 and $BaAl_2Si_2O_8$ from the glass matrix occurs.[11,17] Since secondary phases have not been detected in the $BaTiO_3$ ceramic specimens, we assumed that only the (Ba, Sr)TiO_3 phase with perovskite structure could crystallize. But it is not possible to distinguish the pervoskite phase portions from the glass and the initial $BaTiO_3$ powders based on the microstructure observations.

In addition, as shown in Fig. 4, the Curie point temperature and the sharpness of ferroelectric–paraelectric transition have not changed. Considering that the Curie temperature and the transition peak directly reflect the extent of incorporation and the distribution of the cation incorporated into $BaTiO_3$ lattice,[18] they are much better indicators for substitution of $BaTiO_3$. In other words, there are almost no chemical interactions between the initial $BaTiO_3$ and the glass we have added.

In general, the BDS of ceramics depends on several internal parameters (porosity, grain size and grain boundary nature) and external parameters (sample thickness, sample area, and electrode configuration). We have kept the same external parameters for the BDS measurements. Therefore, the variations in the BDS values cannot be attributed to external effects. Based upon these limited results, it appears that the improvement of the BDS in the glass-added $BaTiO_3$ samples is primarily due to the reduction of grain size in accordance with the microstructure results shown in Fig. 2. Combined Fig. 3 with Fig. 6, it can be seen that for the glass-added $BaTiO_3$ ceramics, there is an increase in the BDS results with decreasing grain size in the range of 1–0.1 μm. This trend was also consistent with $BaTiO_3$ ceramics having grain sizes of about 10 μm, as reported by Tunkasiri and Rujijanagul.[4]

In ceramic materials, the mechanical and electrical strengths show an inverse correlation with the average grain size typically

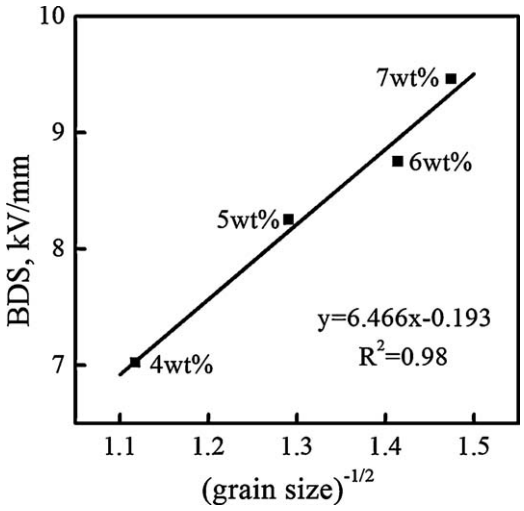

Fig. 13. Dielectric breakdown strength versus (grain size)$^{-1/2}$ for the glass-added $BaTiO_3$ ceramics.

represented by a (grain size)$^{-1/2}$ dependence which relationship is well known for mechanical failure.[5,19] To determine whether the samples fabricated in this study follow this general trend, the relationship between the BDS and the (grain size)$^{-1/2}$ was plotted for the samples that contained different glass contents in Fig. 13. The glass-added $BaTiO_3$ ceramics were found to exhibit the expected trend for the breakdown strength dependence on grain size. The same results were obtained by Beauchamp[19] for the electrical strength of MgO ceramics, by Pohanka et al.[20] for the mechanical fracture strength of $BaTiO_3$ ceramics and Young et al.[5] for breakdown strength of barium titanate ceramics.

4.2. Charge transport contribution

Besides the grain size dependence of the BDS results, the correlation between the BDS results and the difference between bulk and grain boundary activation energies ($\Delta\phi$) was shown in Fig. 14. This result indicates that the dielectric breakdown is related to the charge transport across the grain

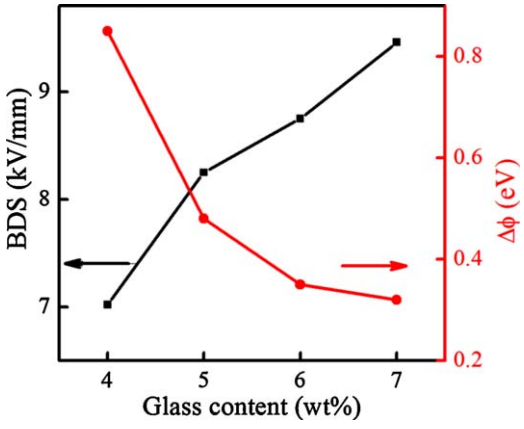

Fig. 14. Dielectric breakdown strength and the difference between bulk and grain boundary activation energies ($\Delta\phi$) as a function of glass concentration.

boundary space–charge depletion layer in the glass-added $BaTiO_3$ ceramics.

Impedance analysis revealed that for the glass-added $BaTiO_3$ ceramics the average grain boundary resistivity is ~1–2 orders of magnitude higher than the corresponding bulk grain resistivity depending on the temperature. These ceramics can be described by an equivalent electrical network that consists of a bulk (*B*) branch and a grain-boundary (GB) branch in terms of a brick-wall model.

A relatively recent question which has arisen is whether the interfacial polarization can have a direct effect on the dielectric breakdown behavior. In ferroelectric glass ceramic materials which have significant interfacial polarization, higher activation energy can result in lower dielectric breakdown strength value.[8] This preliminary result carried out on barium strontium titanate glass ceramics would cause us to hypothesize that an increase in the activation energy of grain boundary suppresses the charge transport across the grain boundary, thereby introducing a higher space charge polarization.

In the present work, the calculated bulk activation energy slightly changes between 0.48 eV and 0.61 eV for the glass-added $BaTiO_3$ ceramics, which might be correlated to the combination of the motion of the first ionization of oxygen vacancies and/or the excitation from other shallow trapping levels present within the band gap of the samples.[21,22] At the same time, when the glass concentration is 4 wt%, the grain boundary activation energy (ϕ_{gb}) shows the value of around 1.33 eV. With increasing glass concentration, the ϕ_{gb} values show somewhat greater variation, from 0.84 eV to 0.93 eV, which means the electrical conduction is predominantly governed by the motion of second ionization of oxygen vacancies.[23,24] In other words, the mobile species in grain boundary are double positively charged oxygen vacancies, while the mobile ones in bulk grain are single positively charged oxygen vacancies or holes.

The difference between the bulk and grain boundary activation energies ($\Delta\phi$) that have been experimentally determined in this work has been used to determine the charge transport across grain boundary, which is useful for the solution of the glass concentration dependence of the BDS results. The change of $\Delta\phi$ with glass concentration will be a good indication of the decrease of the interfacial polarization in the glass-added ceramic system. This is confirmed by the dielectric temperature characteristic curves in Fig. 4, showing the depressed dielectric maximum profiles.

In the BDS measurements, we apply an external field *E* on the sample. Because of the fact that $R_g \ll R_{GB}$, almost the entire field strength falls across the grain boundary region after a certain time, and the bulk can be regarded as virtually field free. The average field strength in the grain boundary space–charge layer, E_{GB}, that results from the external applied field *E* can be obtained from the following equation:[25,26]

$$E_{GB} = E\left(\frac{d_B}{d_{GB}}\right) \tag{8}$$

where d_B denotes the grain size, d_{GB} denotes the width of the grain boundary space charge layer.

With increasing glass concentration, the d_B value decreased, as shown in Fig. 2, while d_{GB} value increase. Hence, the average applied field in the grain boundary space–charge layer decreased. Consequently the substantial increase of BDS values was observed.

4.3. Energy storage properties

Further evidence for the existence of interfacial polarization in the glass-added $BaTiO_3$ ceramics is obtained from the investigation of the *P–E* hysteresis loops. Fig. 12 shows the result of the energy storage density that was calculated from the *P–E* hysteresis loops. The discharged energy density of the ceramics increases in an almost linear fashion with the applied electric field. This relationship contrasts with that of the linear dielectric, in which the electric energy density is proportional to the square of electric field. This difference is related to ferroelectric spontaneous polarization and interfacial polarization which exists in the glass-added $BaTiO_3$ ceramics.

A dramatic impact of the glass concentration on the energy storage density is observed. Modifying the glass concentration only slightly in the $BaTiO_3$ ceramic system again results in a relatively strong effect on energy storage density, as shown in Fig. 12. These results can be explained by the fact that the interfacial polarization is decreased as the glass concentration increases.

5. Conclusions

The effects of different glass concentrations on the microstructures and energy storage properties of the glass-added $BaTiO_3$ ceramics are investigated. The experimental results indicate that with the increase of glass additive concentration, the average grain size reduced remarkably, the temperature dependence of dielectric properties was suppressed at low temperature regime, and the dielectric breakdown strength was notably improved. In addition, the breakdown strength–grain size relationship obeyed the expected parabolic relationship. On the other hand, the correlation between the dielectric breakdown strength and the difference between the bulk and grain boundary activation energies in the glass-added $BaTiO_3$ ceramics is found. The increase of the dielectric breakdown strength is attributed to the decrease of grain size and the improvement of charge transport behavior respectively. Moreover, as the glass concentration increases, the energy storage density of the ceramics increases gradually. This enhancement could be explained by the weakening of interfacial polarization. Thus, controlling grain size and mitigating interface polarization are desirable for the energy storage properties of dielectric ceramics.

Acknowledgements

This work was supported by Tsinghua University Initiative Scientific Research Program and National Natural Science Foundation of China (Grant No. 50977049).

References

1. Freiman SW, Pohanka RC. Review of mechanically related failures of ceramic capacitors and capacitor materials. *J Am Ceram Soc* 1989;**72**(12):2258–63.
2. Huebner W, Zhang SC. High energy density dielectrics for symmetric blumleins. In: *Proceedings of the 12th IEEE International Symposium on Applications of Ferroelectrics, vol. 2*. 2000. p. 833–6.
3. Wu ZH, Liu HX, Cao MH, Shen ZY, Yao ZH, Hao H, Luo DB. Effect of $BaO–Al_2O_3–B_2O_3–SiO_2$ glass additive on densification and dielectric properties of $Ba_{0.3}Sr_{0.7}TiO_3$ ceramics. *J Ceram Soc Jpn* 2008;**116**(2):345–9.
4. Tunkasiri T, Rujijanagul G. Dielectric strength of fine grained barium titanate ceramics. *J Mater Sci Lett* 1996;**15**(20):1767–9.
5. Young A, Hilmas G, Zhang SC, Schwartz RW. Effect of liquid-phase sintering on the breakdown strength of barium titanate. *J Am Ceram Soc* 2007;**90**(5):1504–10.
6. Liebault J, Vallayer J, Goeuriot D, Treheux D, Thevenot F. How the trapping of charges can explain the dielectric breakdown performance of alumina ceramics. *J Eur Ceram Soc* 2001;**21**(3):389–97.
7. Touzin M, Goeuriot D, Guerret-Piécourt C, Juvé D, Fitting HJ. Alumina based ceramics for high-voltage insulation. *J Eur Ceram Soc* 2010;**30**(4):805–17.
8. Huang JJ, Zhang Y, Ma T, Li HT, Zhang LW. Correlation between dielectric breakdown strength and interface polarization in barium strontium titanate glass ceramics. *Appl Phys Lett* 2010;**96**(4):042902.
9. Sarkar SK, Sharma ML. Liquid phase sintering of $BaTiO_3$ by boric oxide (B_2O_3) and lead borate (PbB_2O_4) glasses and its effect on dielectric strength and dielectric constant. *Mater Res Bull* 1989;**24**(7):773–9.
10. Zhang QM, Wang L, Luo J, Tang Q, Du J. Improved energy storage density in barium strontium titanate by addition of $BaO–SiO_2–B_2O_3$ glass. *J Am Ceram Soc* 2009;**92**(8):1871–3.
11. Chen JC, Zhang Y, Deng CS, Dai XM. Effect of the Ba/Ti ratio on the microstructures and dielectric properties of barium titanate-based glass–ceramics. *J Am Ceram Soc* 2009;**92**(6):1350–3.
12. Weibull WJ. A statistical distribution function of wide applicability. *J Appl Mech* 1951;**18**:293–7.
13. Young AL, Hilmas GE, Zhang SC, Schwartz RW. Mechanical vs electrical failure mechanisms in high voltage, high energy density multilayer ceramic capacitors. *J Mater Sci* 2007;**42**:5613–9.
14. Barsoukov E, Macdonald JR. *Impedance spectroscopy: theory, experiment, and applications*. 2nd ed. Hoboken, NJ: Wiley-Interscience; 2005.
15. Guo X, Maier J. Grain boundary blocking effect in zirconia: a schottky barrier analysis. *J Electrochem Soc* 2001;**148**(3):121–6.
16. Yoon SH, Randall CA, Hur KH. Effect of acceptor (Mg) concentration on the resistance degradation behavior in acceptor (Mg)-doped $BaTiO_3$ bulk ceramics. I. Impedance analysis. *J Am Ceram Soc* 2009;**92**(8):1758–65.
17. Zhang Y, Huang JJ, Ma T, Wang XR, Deng CS, Dai XM. Sintering temperature dependence of energy storage properties in $Ba_xSr_{1-x}TiO_3$ glass–ceramics. *J Am Ceram Soc* 2011;**94**(6):1805–10.
18. Wang SF, Yang TCK, Wang YR, Kuromitsu Y. Effect of glass composition on the densification and dielectric properties of $BaTiO_3$ ceramics. *Ceram Int* 2001;**27**(2):157–62.
19. Beauchamp EK. Effect of microstructure on pulse strength of MgO. *J Am Ceram Soc* 1971;**54**(10):484–7.
20. Pohanka RC, Rice RW, Walker Jr BE. Effect of internal stress on the strength of $BaTiO_3$. *J Am Ceram Soc* 1976;**59**(1–2):71–4.
21. Chen A, Zhi Y. High capacitance–temperature sensitivity and giant dielectric constant in $SrTiO_3$. *Appl Phys Lett* 2007;**90**:202903.
22. Xia YD, Liu ZG, Wang Y, Shi L, Chen L. Conduction behavior change responsible for the resistive switching as investigated by complex impedance spectroscopy. *Appl Phy Lett* 2007;**91**(10):102904.
23. Yoon SH, Randall CA, Hur KH. Effect of acceptor (Mg) concentration on the resistance degradation behavior in acceptor (Mg)-doped $BaTiO_3$ bulk ceramics. II. Thermally stimulated depolarization current analysis. *J Am Ceram Soc* 2009;**92**(8):1766–72.
24. Yoon SH, Randall CA, Hur KH. Effect of acceptor concentration on the bulk electrical conduction in acceptor (Mg)-doped $BaTiO_3$. *J Appl Phys* 2010;**107**(10):103721.
25. Vollmann M, Hagenbeck R, Waser R. Grain-boundary defect chemistry of acceptor-doped titanates: inversion layer and low-field conduction. *J Am Ceram Soc* 1997;**80**(9):2301–14.
26. Vollmann M, Waser R. Grain boundary defect chemistry of acceptor-doped titanates: high field effects. *J Electroceram* 1997;**1**(1):51–64.